Investigation of the Iron−Sulfur Cluster in *Mycobacterium tuberculosis* APS Reductase: Implications for Substrate Binding and Catalysis†

Kate S. Carroll,‡,§ Hong Gao,‡,§,|| Huiyi Chen,⊥ Julie A. Leary,|| and Carolyn R. Bertozzi*,§,⊥,#

Departments of Chemistry and Molecular and Cell Biology and Howard Hughes Medical Institute, University of California, Berkeley, California 94702-1460, and Department of Chemistry and Molecular Cell Biology, Genome Center, University of California, Davis, California 95616

Received July 12, 2005; Revised Manuscript Received September 6, 2005

ABSTRACT: The sulfur assimilation pathway is a key metabolic system in prokaryotes that is required for production of cysteine and cofactors such as coenzyme A. In the first step of the pathway, APS reductase catalyzes the reduction of adenosine 5′-phosphosulfate (APS) to adenosine 5′-phosphate (AMP) and sulfite with reducing equivalents from the protein cofactor, thioredoxin. The primary sequence of APS reductase is distinguished by a conserved iron−sulfur cluster motif, -CC-$X_{\sim 80}$-CXXC-. Of the sequence motifs that are associated with 4Fe-4S centers, the cysteine dyad is atypical and has generated discussion with respect to coordination as well as the cluster's larger functional significance. Herein, we have used biochemical, spectroscopic, and mass spectrometry analysis to investigate the iron−sulfur cluster and its role in the mechanism of *Mycobacterium tuberculosis* APS reductase. Site-directed mutagenesis of any cysteine residue within the conserved motif led to a loss of cluster with a concomitant loss in catalytic activity, while secondary structure was preserved. Studies of 4Fe-4S cluster stability and cysteine reactivity in the presence and absence of substrates, and in the free enzyme versus the covalent enzyme−intermediate (E-Cys-S-SO_3^-), suggest a structural rearrangement that occurs during the catalytic cycle. Taken together, these results demonstrate that the active site functionally communicates with the iron−sulfur cluster and also suggest a functional significance for the cysteine dyad in promoting site differentiation within the 4Fe-4S cluster.

In mammals, cysteine is formed from the catabolism of the essential amino acid methionine. By contrast, many bacteria synthesize cysteine de novo through nucleophilic displacement of acetate from *O*-acetylserine with sulfide. Since mammals lack the machinery to generate the reduced sulfur required for cysteine biosynthesis, bacterial enzymes that participate in sulfate reduction represent attractive targets for therapeutic intervention. Toward this end, our laboratory has focused attention on enzymes that comprise the sulfate assimilation pathway in the human pathogen *Mycobacterium tuberculosis* (Figure 1) (*1*−*3*).

The first committed step in the biosynthesis of cysteine in mycobacteria is catalyzed by APS reductase (*3*). In this reaction, activated sulfate in the form of adenosine 5′-phosphosulfate (APS)[1] is reduced to sulfite and adenosine 5′-phosphate (AMP) using reduction potential supplied by the protein cofactor, thioredoxin (Trx) (Scheme 1). Notably, APS reductase has been identified in a screen for essential genes in *Mycobacterium bovis* (*4*) and is critical for virulence in a murine model of tuberculosis infection (R. Senaratne, personal communication).

Not all organisms that assimilate sulfate reduce APS as a source of sulfite. Through divergent evolution some organisms such as *Escherichia coli* and *Saccharomyces cerevisiae* reduce the related metabolite 3′-phosphoadenosine 5′-phos-

Scheme 1: Reaction Catalyzed by Sulfonucleotide Reductases

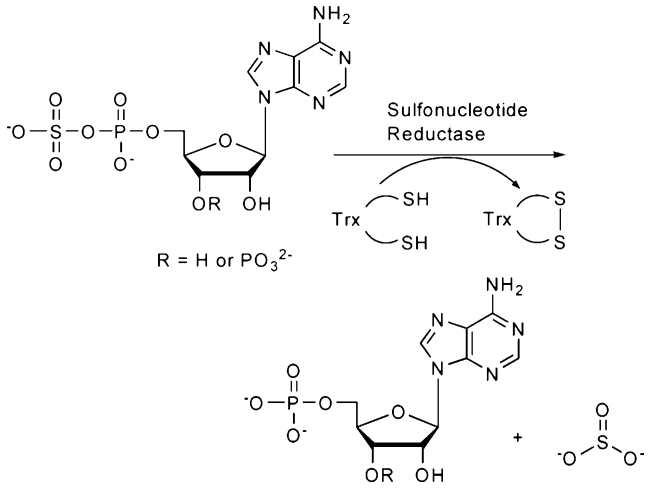

† This work was funded by a grant from the National Institutes of Health to C.R.B. K.S.C. is a Damon Runyon Fellow supported by the Damon Runyon Cancer Research Foundation (DRG-1783-03).

* Correspondence should be addressed to this author. Phone: 510-643-1682 Fax: 510-643-2628. E-mail: crb@berkeley.edu.

‡ These authors contributed equally to this work.

§ Department of Chemistry, University of California, Berkeley.

|| Department of Chemistry and Molecular Cell Biology, University of California, Davis.

⊥ Department of Molecular and Cell Biology, University of California, Berkeley.

Howard Hughes Medical Institute, University of California, Berkeley.

10.1021/bi051344a CCC: $30.25
Published on Web 10/14/2005

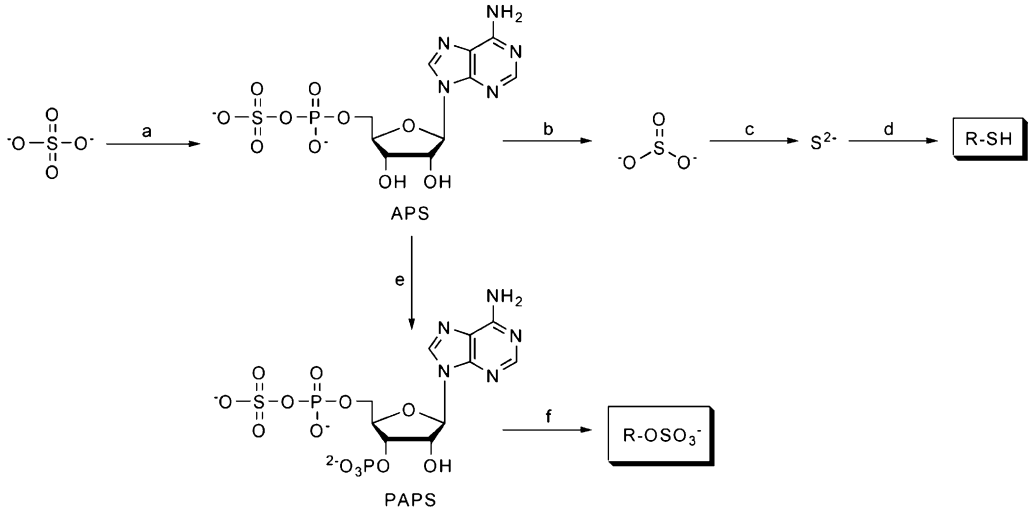

FIGURE 1: Sulfate assimilation pathway in *M. tuberculosis*. Inorganic sulfate is adenylated by ATP sulfurylase (a) to form APS. In the next step, APS is reduced to sulfite by APS reductase (b). Sulfite is reduced to sulfide by sulfite reductase (c) and incorporated into cysteine by *O*-acetylserine-(thiol) lyase (d). Important metabolites such as methionine and coenzyme A are, in turn, synthesized from cysteine. Alternatively, APS can be phosphorylated a second time by APS kinase (e) to form PAPS, the universal sulfate donor. Sulfotransferases (f) use PAPS to sulfate various metabolites.

FIGURE 2: Cysteine residues of *M. tuberculosis* APS reductase. With the exception of C59, each cysteine is located in the sulfonucleotide reductase domain (shown in gray). C140, C141, C223, and C226 comprise the iron−sulfur cluster motif, and C249 is an essential catalytic nucleophile.

phosulfate (PAPS) (Scheme 1) (*5*−*7*). In recent work, we have reported a mechanistic investigation of sulfonucleotide reductases as a class of enzymes (*8*). These data support a two-step mechanism in which the sulfonucleotide undergoes nucleophilic attack to form an enzyme−thiosulfonate (E-Cys-S-SO_3^-) intermediate (Scheme 2). Sulfite is then released in a thioredoxin-dependent manner (*8*).

The primary sequence of assimilatory APS reductases is distinguished by the presence of the conserved cysteine motif, -CC-$X_{\sim 80}$-CXXC- (Figure 2). Mössbauer spectroscopy, in combination with quantitative analysis of iron and sulfide content, has established a stoichiometry of four iron and four sulfur atoms (4Fe-4S) for this cluster (*6*, *9*, *10*). Interestingly, the Mössbauer spectra of *Arabidopsis thaliana* and *Pseudomonas aeruginosa* APS reductases present as an asymmetric quadrupole doublet. Unlike the prototypical [4Fe-4S]$^{2+}$ cluster in which the four iron sites are equivalent in geometry and valence, the data collected with APS reductase indicate that there are structural differences among the four iron sites (*6*, *9*). One possibility proposed by Kopriva et al. and Kim et al. is that the iron−sulfur cluster has only three cysteinyl ligands (*9*, *10*). However, other models of coordination could also account for the observed Mössbauer parameters. Thus, the details of cysteine ligation remain to be established.

Another fundamental question that remains unanswered is what role does the iron−sulfur cluster play in APS reductase? Central to this question is the fact that PAPS reductases have lost the cysteine motif and, therefore, do not possess an iron−sulfur cofactor (*6*). This interesting evolutionary twist has prompted some to conclude that the cluster plays only a structural or regulatory role (*11*). Alternatively, it has also been proposed that the iron−sulfur cluster might perform a catalytic function during APS reduction (*8*, *10*).

Scheme 2: Mechanism of Sulfonucleotide Reduction

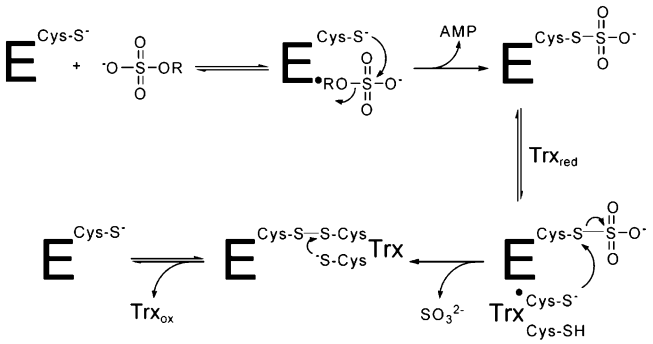

Here, a combination of biochemical, spectroscopic, and ESI FT-ICR mass spectrometry approaches has been used to investigate the iron−sulfur cluster and mechanism of *M. tuberculosis* APS reductase. We demonstrate that APS reductase activity is intimately linked to the 4Fe-4S cluster and present data that strongly suggest a role in coordination for all four cysteines in the cluster motif. Further, differences in cysteine reactivity and cluster stability suggest a structural rearrangement in the covalent enzyme−intermediate and AMP-bound enzyme relative to the free enzyme. These results indicate that the iron−sulfur cluster is a key constituent of the active site and also suggest a functional significance for the cysteine dyad in promoting site differentiation within the 4Fe-4S cluster.

MATERIALS AND METHODS

Materials. Nonradioactive APS was purchased from Biolog Life Sciences Institute, ≥95% (Bremen, Germany).

[1] Abbreviations: AMP, adenosine 5′-phosphate; APS, adenosine 5′-phosphosulfate; NH_4OAc, ammonium acetate; DTT, dithiothreitol; E, enzyme; 4Fe-4S, four iron−four sulfur cluster; FT-ICR, Fourier transform ion-cyclotron resonance; ICP, inductively coupled plasma; IDA, iodoacetamide; OBP, *o*-bathophenanthrolinedisulfonate; PAPS, 3′-phosphoadenosine 5′-phosphosulfate; S, substrate; TLC, thin-layer chromatography; Trx, thioredoxin; ESI, electrospray ionization.

[^{35}S]SO_4^{2-} (specific activity 1491 Ci/mmol) was obtained from MP Biochemicals (Irvine, CA). Molecular biology grade DTT was from Invitrogen (Carlsbad, CA). *E. coli* thioredoxin protein was purchased from EMD Biosciences (San Diego, CA). Iodoacetamide was from Sigma (Sigma-Aldrich, St. Louis, MO). Depending upon availability, PEI−cellulose TLC plates (20 cm × 20 cm) were purchased from J. T. Baker (Phillipsburg, NJ) or EMD Biosciences. Pfu and DpnI polymerase were from Stratagene (La Jolla, CA). DNA oligonucleotides were purchased from Qiagen (Valencia, CA). ^{35}S-Labeled APS and PAPS were prepared by incubating [^{35}S]Na_2SO_4, ATP, ATP sulfurylase (Sigma), inorganic pyrophosphatase (Sigma), and recombinant APS kinase together as previously described (*8*). All other chemicals were purchased from J. T. Baker and were of the highest purity available (≥95%).

Biochemical Methods. (A) Site-Directed Mutagenesis of APS Reductase. The protein expression vector containing *M. tuberculosis* APS reductase was prepared as described previously (*3*). Site-specific mutations were made using the QuikChange PCR mutagenesis kit (Stratagene) using the appropriate plasmid template according to the manufacturer's specifications. Successful incorporation of the desired mutation was confirmed by DNA sequencing.

(B) Genetic Complementation in E. coli. The gene encoding *M. tuberculosis* APS reductase was cloned into pUC18/RBS as previously described (*3*). Plasmid DNA was transformed into *E. coli* JM96 by electroporation. Transformants were grown on CM1-agarose (1 g of Oxoid Lab Lemco powder, 2 g of yeast extract, 5 g of peptone, and 5 g of NaCl per liter) containing 100 mg/L ampicillin before transfer to M9 minimal medium containing $MgSO_4$ as the sole sulfur source as previously described (*3*).

(C) Expression and Purification of APS Reductases. Wild-type, C59S, and C249S proteins were produced in *E. coli* BL21(DE3) (Novagen). The remaining proteins were produced in BL21(DE3) Rosetta cells (Novagen). Wild-type and variant *M. tuberculosis* APS reductase proteins were purified as previously described (*8*). Protein concentration was determined by quantitative amino acid analysis (AAA Service Laboratory, Boring, OR). Iron content of each protein preparation was determined in triplicate by inductively coupled plasma (ICP) analysis and also by colorimetric assay as previously described (*12*, *13*).

General Kinetic Analysis. APS reduction reactions were performed at 30 °C in assay buffer (50 mM sodium phosphate, pH 7.0, adjusted to 100 mM ionic strength with NaCl) as previously described (*8*). Nonradioactive APS was doped with a trace amount of [^{35}S]APS. Reactions contained 5−100 nM APS reductase, 25 μM APS, 10 μM thioredoxin, and 5 mM DTT and were typically initiated by the addition of APS. The products and unreacted substrate were separated by TLC on PEI−cellulose plates and developed in 1 M LiCl and 0.3 M sodium phosphate, pH 3.8. TLC plates were analyzed by phosphorimaging (Molecular Dynamics) with Image Quant quantitation software. With the exception of very slow or undetectable reactions, the enzymatic reactions were monitored to completion (≥5 half-lives). The initial linear portion of the reaction (≤15% reaction) was used to calculate the reaction rate. The resulting rate was then divided by enzyme concentration to yield k_{rxn}. Kinetic data were measured in at least three independent experiments.

Iron Chelation and Alkylation of Cysteines. Cysteine alkylation of 1 mg/mL APS reductase was carried out in gel filtration buffer (50 mM Tris-HCl, pH 8.0, 10% glycerol, and 5 mM DTT and ionic strength adjusted to 150 mM with NaCl) with iodoacetamide at a final concentration of 25 mM. To chelate iron, *o*-bathophenanthrolinedisulfonate (OBP) was added at a final concentration of 125 mM. The chelation of iron was monitored by the absorbance increase at 535 nm, and the quantity of iron chelated was determined using an extinction coefficient of 22140 M^{-1} cm^{-1} (*14*). Reactions were typically allowed to proceed at room temperature for 1 h. In control reactions in which the chelating and labeling times were extended, no differences in the pattern of alkylation were observed. Furthermore, no differences in alkylation patterns were observed when DTT was omitted. Some reactions included APS or AMP. In this case, ligand was incubated with enzyme for 15 min on ice prior to the addition of iodoacetamide and OBP. The specific concentration of these ligands in each experiment is reported in the corresponding figure legend.

Spectroscopic Methods. UV−visible absorption spectra were recorded using a Uvikon spectrophotometer. X-band electron paramagnetic resonance (EPR) spectra were recorded on a Varian E-109 spectrometer with an E-102 microwave bridge. Samples were measured at 6 K using an Air Products Heli-tran liquid helium cryostat. Circular dichroism (CD) spectra were collected on an Aviv 62DS spectropolarimeter (Aviv Associates, Lakewood, NJ) in a 1 cm path length cuvette at 4 and 25 °C. Protein was analyzed between 0.03 and 0.07 mg/mL in 10 mM sodium phosphate, pH 7.0. Data points were recorded from 260 to 200 nm, at 1 nm intervals. Each data point was averaged for 5 s. For each sample, a total of five scans were recorded and averaged to obtain the final spectrum. As the unfolded reference, samples were denatured in 5 M guanidine hydrochloride.

Sample Preparation for Mass Spectrometry. Aliquots of purified APS reductase or thioredoxin were exchanged into 50 mM ammonium acetate (NH_4OAc) buffer, pH 7.5, using Amicon 10000 Da molecular mass cutoff centrifugal filters with the temperature of the centrifuge set at 4 °C as previously described (*8*). OBP-treated and iodoacetamide-labeled samples were also exchanged into NH_4OAc buffer to remove small molecule reagents and then diluted with 80:20 acetonitrile:water containing 1% formic acid for mass analysis.

Mass Spectrometry. Mass spectrometry data were acquired on a Bruker Fourier transform ion cyclotron resonance (FT-ICR) mass spectrometer equipped with an actively shielded 7 T superconducting magnet as previously described (*8*). Briefly, solutions were infused at a rate of 2 μL/min into an Apollo electrospray source (Bruker, Billerica, MA) operated in the positive mode. All ions were collected using gated trapping and detected using chirp excitation. Broad band data were acquired using an average of 16−64 time domain transients containing 32 K or 1 M data points. The original time domain free induction decay (FID) spectra were zero filled, Gaussian multiplied, and Fourier transformed. All the data were acquired and processed using Bruker Xmass version 6.0.0 software (Billerica, MA). The parameters of the electrospray ionization (ESI) source, ion optics, and cell were tuned for the best signal-to-noise ratio and were maintained for systematic experiments.

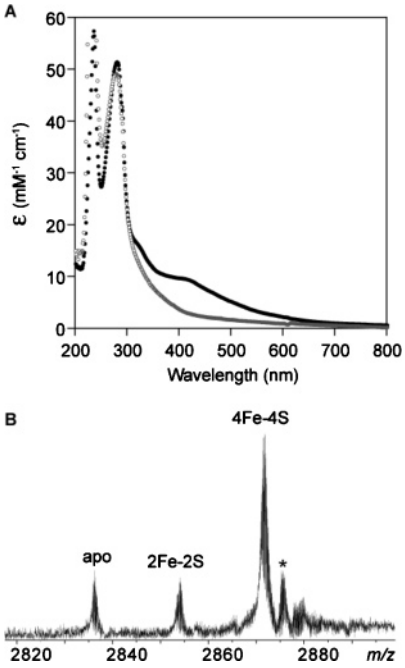

FIGURE 3: Optical and ESI FT-ICR spectra of *M. tuberculosis* APS reductase. (A) UV−visible absorption spectra of 10 μM APS reductase associated with (●) or without (○) an iron−sulfur cofactor. Formation of the thiosulfonate−enzyme intermediate permitted the absorption spectrum of the 4Fe-4S to persist, consistent with other data presented in this work (not shown). No other significant changes in the absorption spectrum upon formation of the intermediate were observed, due to the broad absorption features exhibited by the cluster. (B) ESI FT-ICR mass spectrum of 10 μM APS reductase in 50 mM NH_4OAc, pH 7.5. Expansion of the 10+ charge state showing ions that correspond to apoprotein, a 2Fe-2S intermediate, and the holoenzyme (complete 4Fe-4S cluster). The satellite ion marked with an asterisk is 64 Da higher than the holoenzyme. The molecular mass of this adduct most closely corresponds to the expected molecular mass of two sulfide−protein adducts. Such adducts are common in samples that contain free sulfide due to oxidation and dissociation of iron−sulfur clusters (*18*).

RESULTS

The iron−sulfur cluster in *M. tuberculosis* APS reductase was initially characterized by UV−visible absorption and quantitative analysis of iron content. In addition to aromatic amino acid absorption at 280 nm, the UV−visible spectrum of APS reductase exhibited an absorption centered at 410 nm, which is characteristic of iron−sulfur proteins (Figure 3A, closed circles). The extinction coefficient at 410 nm (ϵ^{410}) was 10470 M^{-1} cm^{-1}. Analysis of total iron content for wild-type APS reductase indicated that each mole of protein contained 3.8 mol of iron (Table 1).

Electrospray FT-ICR mass spectrometry was also used to probe the stoichiometry and oxidation state of the iron−sulfur cluster in *M. tuberculosis* APS reductase. The ESI conditions necessary to retain noncovalently associated complexes, including iron−sulfur centers, have been previously described (*15*, *16*). Moreover, the high resolving power of FT-ICR mass spectrometry allows for the detection of small mass changes such as those associated with disulfides as well as changes in cluster oxidation state (*17*, *18*). In our mass analysis of APS reductase, the enzyme was sprayed directly from ammonium acetate buffer that allows for the observation of the folded protein. The resulting spectrum for the +10 charge state of APS reductase is shown in Figure 3B.

Table 1: Analysis of Activity and Iron Content for Wild-Type *M. tuberculosis* APS Reductase and Its Variants[a]

	k_{rxn} (s^{-1})[b]	iron content (mol of iron/mol of protein)
wild type	2.4 ± 0.6	3.82 ± 0.02
C59S	1.4 ± 0.3	3.59 ± 0.02
C140S	ND	0.04 ± 0.01
C141S	ND	0.01 ± 0.01
C223S	ND	0.02 ± 0.01
C226S	ND	0.01 ± 0.01
C249S	ND	3.67 ± 0.05

[a] 0.1 M sodium phosphate, pH 7.0, and 100 mM NaCl at 30 °C. [b] No detectable catalytic activity (ND).

The deconvoluted mass of APS reductase was measured to be 28705.97 Da. This value was in excellent agreement with the calculated mass for APS reductase associated with four irons, four sulfurs, and a cluster oxidation state of 2+ (28705.95 Da). The diamagnetic nature of the cluster was verified using electron paramagnetic resonance (EPR) spectroscopy. *M. tuberculosis* APS reductase exhibited a minor EPR signal that was centered near $g = 2.01$ (data not shown). The EPR signal corresponded to less than 0.01 spin/mol of enzyme and is consistent with data previously reported for *P. aeruginosa*, *Lemina minor*, and *A. thaliana* APS reductases (*9*, *10*). No significant change in the EPR spectrum was observed in the presence of strong reducing reagents, with thioredoxin, or in the context of the thiosulfonate enzyme−intermediate (data not shown).

In our mass spectrum of APS reductase we also observed two series of ions at lower mass to charge ratio corresponding to apo and 2Fe-2S APS reductase (Figure 3B). The masses of these proteins were 28352.4 and 28529.3 Da, respectively. The mass of apo APS reductase was four mass units lower than the calculated molecular mass of 28356.2 Da. This mass difference most likely resulted from the formation of disulfide bonds. Using a combination of site-directed mutagenesis and mass spectrometry, we have previously demonstrated that C59 and C249 are not involved in disulfide formation in holo or apo APS reductase (*8*). Since the protein's folded form is retained under the conditions of our analysis, the complete dissociation of the iron−sulfur cluster from APS reductase leaves four cysteine residues (Figure 2: C140, C141, C223, and C226) together in close proximity to form two disulfide bonds. Disulfide formation between cysteinyl ligands has also been observed for other iron−sulfur proteins (*17*, *18*). The mass of 2Fe-2S APS reductase was two mass units lower than the calculated molecular mass of 28531.3 Da, consistent with an oxidation state of 2+ for this cluster. In addition to the excellent mass agreement, data reported by Berdnt et al. provide further support for our assignment of the 2Fe-2S APS reductase ion. In this work, a form of *Bacillus subtilis* sulfonucleotide reductase was observed with spectral properties consistent with those of a 2Fe-2S cluster (*11*). Finally, the stability of the iron−sulfur cluster during gas-phase dissociation was also investigated. The results indicated that the apo and 2Fe-2S forms of APS reductase were not generated during the electrospray process (Gao et al., manuscript in preparation).

Iron Content and Activity of Wild-Type APS Reductase and Its Variants. The primary sequence of *M. tuberculosis* APS reductase contains six cysteines (Figure 2). The

C-terminal cysteine, C249, is an essential nucleophile and is conserved among all sulfonucleotide reductases (Scheme 2). Of the five remaining cysteines, four are conserved among APS reductases and comprise the iron−sulfur cluster motif: C140, C141, C223, and C226. The sixth cysteine, C59, is dispensable for catalysis, consistent with its lack of conservation in this family of enzymes (*8*).

Each cysteine in *M. tuberculosis* APS reductase was individually changed to serine, and the resulting variants were evaluated in vitro for their ability to incorporate iron and catalyze APS reduction (Table 1). For these studies, each protein was purified in two steps using affinity and size-exclusion chromatography. Gel filtration analysis of *M. tuberculosis* APS reductase cluster variants revealed that the majority of the protein was aggregated, with a molecular mass ≥600 kDa. The remaining protein (10−20%) migrated with the expected molecular mass, ∼28.7 kDa. A comparison of iron and protein content revealed that the aggregated material was associated with a disproportionate amount of iron relative to the nonaggregated protein. Nonetheless, the aggregated protein was not associated with any detectable catalytic activity (data not shown). In the work reported here, we have confined our studies to the nonaggregated protein for analysis of iron content, activity, and structure. By contrast, analysis of iron content and activity reported in previous studies with *A. thaliana* and *P. aeruginosa* enriched APS reductase solely by affinity chromatography (*9*, *10*).

All six mutations had a deleterious effect on the amount of iron associated with the enzyme (Table 1). However, mutations of cluster motif cysteines yielded the most drastic effect, incorporating ≤1.5% iron relative to wild type. C249S and C59S variants incorporated 3.7 and 3.6 mol of iron/mol of protein, respectively. An established TLC-based assay was used to quantify the ability of these proteins to catalyze APS reduction (Table 1) (*8*, *19*). No detectable catalytic activity was observed for the C140S, C141S, C223S, and C226S variants. Likewise, no catalytic activity was detected for C249S. Consistent with data reported earlier, the C59S variant exhibited only a minor defect in activity relative to the other serine variants in this study, with $k_{rxn} = 1.4\ s^{-1}$ as compared to $2.4\ s^{-1}$ for wild type (*8*). This difference in activity is most likely due to fewer active enzyme molecules in the C59S sample, consistent with the modest decrease in its iron content. In addition, we tested whether the mutations affected the function of the protein in vivo. A plasmid encoding wild-type and C59S *M. tuberculosis* APS reductase was able to complement *E. coli* JM96 (a mutant strain lacking PAPS reductase); the five remaining variants did not complement *E. coli* JM96.

Cysteine Reactivity of M. tuberculosis APS Reductase. Mutation of any cysteine within the cluster motif had the greatest impact on iron content, consistent with an important role in iron−sulfur cluster ligation. As an independent test of cluster ligand identity, the reactivity of cysteines following cluster removal was also investigated. The iron chelating reagent, *o*-bathophenanthrolinedisulfonate (OBP) has been used previously to selectively extrude the iron−sulfur cluster and facilitate ligand identification (*14*). If each of the cysteines were involved in cluster ligation, the simplest prediction is that removal of the cluster would render these four cysteines accessible to thiol-labeling reagents, such as iodoacetamide.

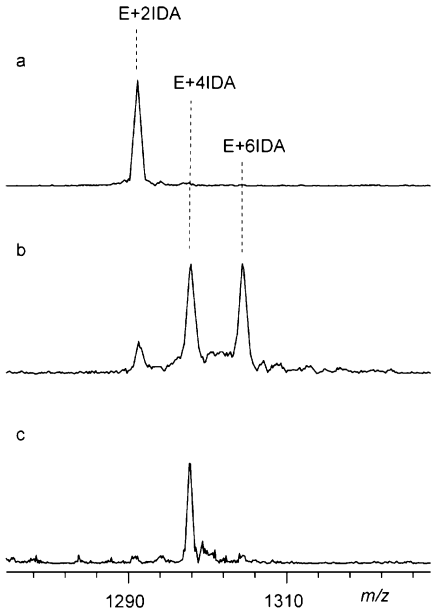

FIGURE 4: Reaction of APS reductase cysteines with iodoacetamide during OBP chelation. Expansion of the 22+ charge state of the ESI FT-ICR mass spectra. APS reductase (E) was reacted with 0 mM (a) or 125 mM (b) OBP or preincubated with AMP and reacted with 125 mM OBP (c). Each sample was alkylated using 25 mM iodoacetamide (IDA). The total number of covalently modified cysteines was determined by analyzing the sample in 80:20 acetonitrile:water containing 1% formic acid as described in the Materials and Methods section.

Alkylation of *M. tuberculosis* APS reductase in the absence of the cluster chelator yielded a single species with the measured mass of 28468.4 Da, two mass units less than the calculated mass expected for APS reductase with two covalent iodoacetamide modifications, 28470.3 Da (Figure 4a). Using a combination of site-directed mutagenesis and mass analysis, the identity of these alkylated cysteines was established as the nonconserved N-terminal cysteine, C59, and the essential nucleophile, C249 (*8*). In these experiments, after buffer exchange to remove excess labeling reagent, we analyzed the sample in organic solvent to probe for covalent modifications to APS reductase, as described in the Materials and Methods section. This analysis results in the dissociation of any noncovalently bound protein ligands, including the iron−sulfur cluster. The mass shift of −2 Da observed in this analysis would be consistent with the formation of a disulfide between two cysteine residues in the cluster motif in the absence of the metal center.

To probe for changes in cysteine reactivity in the absence of the iron−sulfur cluster, OBP was included in the alkylation reaction. Analysis of the reaction products indicated that there were two major species with masses that corresponded to APS reductase alkylated at four and six cysteine residues (Figure 4b). Trypsin digestion of this sample followed by peptide mapping confirmed that only cysteine-containing peptides were alkylated (data not shown). Therefore, each of the putative cluster ligands was alkylated when the iron−sulfur cluster was removed from APS reductase.

Notably, although these reactions were carried out under reducing conditions, the mass of the protein alkylated at four cysteines was 28582.3 ± 0.2 Da. This value is two mass units lower than the calculated mass of 28584.3 Da. Since C59 and C249 are always alkylated (*8*), this mass difference

suggested that a disulfide bond had formed between two cysteines within the cluster motif, thereby precluding their alkylation. Further analysis of this protein via peptide mapping indicated that C223 and C226 were always fully alkylated, while C140 and C141 were only partially alkylated (data not shown). Since a significant fraction of protein that was alkylated at all six cysteine residues was also observed in these reactions, these data suggest that when the iron−sulfur cluster was removed, the alkylation reaction competed with disulfide formation between cluster motif residues, C140 and C141.

Intermediate Formation and AMP Binding Alter Thiol Reactivity. Previous studies have reported that ligand binding to iron−sulfur proteins influences their cysteine reactivity, thereby providing evidence for conformational change (*20*). In light of this work, we wondered whether ligand binding prior to the removal of the iron−sulfur cluster might also alter the cysteine reactivity in APS reductase. To test this possibility, APS reductase was incubated with AMP to form a binary complex. In a subsequent step, OBP and iodoacetamide were added to remove the iron−sulfur cluster and modify free thiols. In contrast to the distribution between four and six alkylations observed for free enzyme, only a single species with a mass of 28582.3 Da was observed (Figure 4c). This mass was in excellent agreement with the calculated mass for APS reductase alkylated at four cysteines with one disulfide bond, 28582.4 Da. On the basis of UV absorbance, the addition of AMP did not reduce the total amount of iron chelated, indicating that the observed decrease in alkylation was not due to decreased cluster accessibility or a discrepancy in the quantity of iron that was removed (data not shown). Therefore, the simplest interpretation of these data is that AMP binding resulted in a conformational change that facilitated disulfide formation between C140 and C141. The same experiment was performed with APS reductase that had been preincubated with APS to form the thiosulfonate enzyme−intermediate. Formation of this intermediate was confirmed by the observation of a +80 Da mass shift by mass analysis (*8*). However, when OBP and iodoacetamide were added to the thiosulfonate enzyme−intermediate, we no longer observed the +80 Da mass shift, indicating that the covalently bound sulfite had been lost (data not shown).

Sulfonic acid ($R-SO_3H$) has been previously demonstrated to release covalently bound sulfite from APS reductase (*8*, *21*). Therefore, the loss of the covalent adduct was most likely due to the sulfonic acid moieties of OBP. To test this hypothesis, OBP was omitted from the alkylation reaction of the thiosulfonate enzyme−intermediate. The mass of the resulting protein was 28493.1 Da, in excellent agreement with the calculated mass for APS reductase with one alkylation and one sulfite modification. Again, using site-directed mutagenesis and mass analysis, we have previously established that the alkylation occurs at C59 and sulfite attachment at C249 (*8*). From these data, we conclude that OBP was responsible for the observed sulfite release. An additional interesting observation made in this experiment was that, unlike free enzyme, no disulfide bonds were formed between liberated cysteinyl ligands in the thiosulfonate enzyme−intermediate when the iron−sulfur cluster was dissociated under the conditions of the mass analysis; the mass of the intermediate was 28493.1 Da compared to the calculated value of 28493.3 Da. Consistent with this observation, a comparison of peptide maps derived from free and thiosulfonate-bound enzyme that had been denatured in urea and labeled with iodoacetamide revealed that C140 and C141 were alkylated in the thiosulfonate intermediate but not in free enzyme (data not shown). Furthermore, comparison of the trypsin digestion patterns for folded APS reductase and its intermediate by SDS−PAGE indicated that the thiosulfonate enzyme−intermediate was almost entirely protected from cleavage as compared to the free enzyme (data not shown). Taken together, these data suggest that the thiosulfonate enzyme−intermediate also differed in conformation from the unbound catalyst.

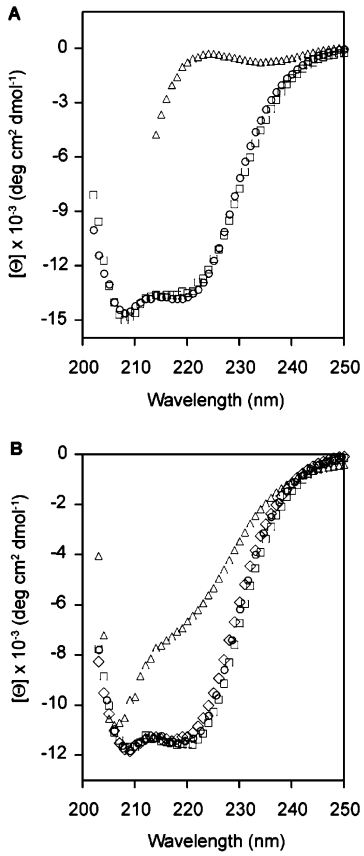

FIGURE 5: Circular dichroism spectra for wild-type APS reductase and its variants. Proteins were analyzed in 10 mM sodium phosphate, pH 7.0 at 4 °C. (A) Wild-type (○), C223S (□), and APS reductase unfolded in 5 M guanidine hydrochloride (△). (B) Wild-type (○), C249S (□), C59S (◇), and apo APS reductase incubated at room temperature for 1 week (△). Minor variation in spectra was observed between independent experiments. Therefore, wild-type APS reductase was always included as a standard for comparison.

Probing Secondary Structure in APS Reductase. To determine if loss of the iron−sulfur cluster led to unfolding and defects in secondary structure, the circular dichroism (CD) spectra of wild-type APS reductase and serine variants were analyzed. For wild-type enzyme, a signal consistent with α-helix character was observed, including a strong negative absorption at 208 nm (Figure 5A). A slightly shallower signal was observed at 222 nm. This observation would be consistent with the presence of β structure in combination with α-helix character. Surprisingly, the CD spectrum of C223S, a protein devoid of iron (Table 1), was essentially identical to wild-type enzyme (Figure 5A). Similar results were obtained for C140S and C141S, although the

absorbance at 222 nm was less intense (data not shown). In contrast to wild type and the cluster variants, APS reductase that was unfolded in 5 M guanidine hydrochloride exhibited no significant secondary structure (Figure 5A). The CD spectra of the C59S and C249S were also examined and compared to wild type. The spectra of these variants overlapped with the spectrum of wild-type APS reductase (Figure 5B). Finally, the CD spectrum of wild-type APS reductase, incubated at room temperature for 1 week, was also measured. Under these conditions, the iron−sulfur cluster dissociates from the protein scaffold to form the apoenzyme (see below Figure 8). In contrast to the serine variants that were analyzed within hours of thawing, this sample exhibited a significant degree of unfolding. This observation is consistent with a time-dependent decrease in the stability of secondary structure in the apoprotein.

The 4Fe-4S Cluster Is Essential for Ligand Association. Previous work indicates that APS reductase requires an intact 4Fe-4S cluster for thiosulfonate enzyme−intermediate formation (*8*). Two explanations for these data can be proposed. First, it is possible that the iron−sulfur cluster is essential for substrate binding, through a direct interaction or indirectly through preorganization of the enzyme active site. Alternatively, APS could bind in the absence of the cluster but not undergo the first chemical step to form the covalent intermediate. To distinguish between these models, we tested the ability of APS reductase to bind ligands by mass spectrometry.

The majority of the APS reductase protein preparation was associated with a complete 4Fe-4S cluster (Table 1 and Figure 3B). Nonetheless, iron−sulfur cluster oxidation occurred under aerobic conditions. Therefore, as discussed above, ions corresponding to apo and 2Fe-2S APS reductases were all components of our protein preparation (Figure 3B). Mass analysis enabled the independent evaluation of the behavior of each form of APS reductase by monitoring these ions for the appropriate mass shift upon the addition of ligand.

The concentration of APS reductase required for mass analysis resulted in rapid formation of the thiosulfonate enzyme−intermediate ($k_{rxn} \geq 2\ s^{-1}$). As a result, the time resolution of these experiments did not enable detection of the binary complex between APS and APS reductase. Therefore, as an alternative probe for ligand interaction we investigated the ability of holoenzyme, 2Fe-2S, and apo forms of APS reductase (Figure 6A) to interact with AMP or thioredoxin. Incubation of AMP with APS reductase yielded the expected +347 Da shift for the holoenzyme (Figure 6B). In addition, a binary complex was observed between thioredoxin and APS reductase holoenzyme (Figure 6C). In contrast, ions of APS reductase that lacked a mature iron−sulfur cluster did not exhibit a corresponding mass shift in the presence of either ligand (Figure 6B,C).

Activity Loss and Fe-S Cluster Oxidation Are Prevented by Thiosulfonate Enzyme−Intermediate Formation. Consistent with other reported observations with APS reductases from other organisms, all proteins examined in this study exhibited time-dependent cluster oxidation and dissociation from the protein scaffold (*9*, *11*). Loss of cluster could be monitored qualitatively by the obvious loss of brown color associated with APS reductase or quantitatively via loss of absorption at 410 nm (Figure 3A, open circles). The

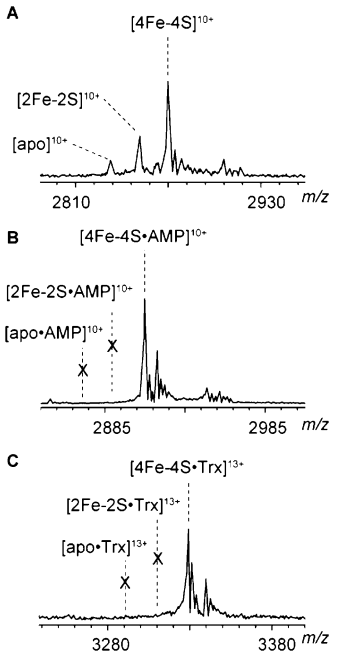

FIGURE 6: The 4Fe-4S cluster is required for binding to AMP and thioredoxin. ESI FT-ICR mass spectra obtained for 10 μM APS reductase in the absence (A) and presence of 25 μM AMP (B) or 2.5 μM thioredoxin (Trx) (C).

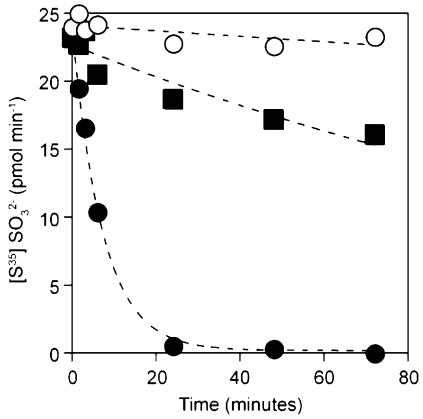

FIGURE 7: Stability of *M. tuberculosis* APS reductase activity. Recombinant APS reductase (10 μM) was purified and stored under aerobic conditions at 4 °C for a total of 3 days alone (●), with 1 mM AMP (■), or with 100 μM APS (○). At the indicated times, a final concentration of 5 nM APS reductase was analyzed for its ability to catalyze APS reduction.

dissociation of the iron−sulfur cluster from APS reductase clearly has functional consequences since it correlates strongly with a loss of catalytic activity (Table 1 and refs *9*, *11*, and *22*). In a Tris buffer under aerobic conditions, a kinetic analysis of catalytic activity indicated that the half-life of *M. tuberculosis* APS reductase was less than 5 h (Figure 7, closed circles).

Previously, we have demonstrated that incubation of APS with APS reductase results in the formation of a stable thiosulfonate enzyme−intermediate; reduction of this intermediate to form product is a thioredoxin-dependent process (Scheme 2) (*8*). Further, the data presented above suggest that the thiosulfonate-bound intermediate differs in conformation from the free enzyme. Therefore, we also tested the catalytic stability of APS reductase as the covalent intermediate. Strikingly, formation of the thiosulfonate enzyme−

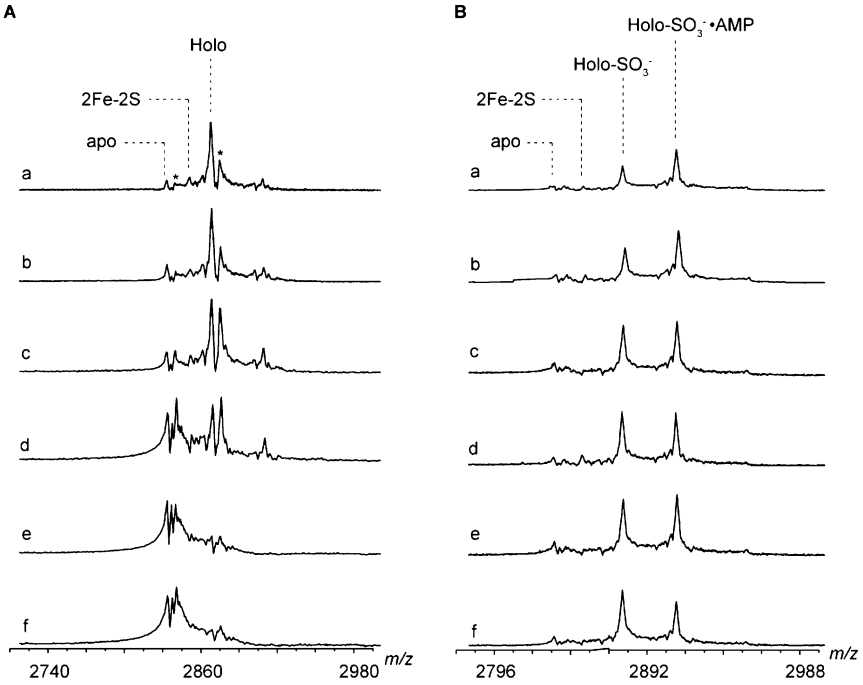

FIGURE 8: Stability of the *M. tuberculosis* APS reductase iron−sulfur cluster. ESI FT-ICR mass spectra of APS reductase in the absence (A) or presence (B) of a 10 molar excess of APS. Expansion of the 10+ charge state of the mass spectra. Reactions were incubated on ice; from a to f, incubation time was 0, 1, 2, 3, 4, and 5 h. Adducts of inorganic sulfide are indicated by an asterisk; see text for details.

intermediate prevented the loss of APS reductase activity over 72 h (Figure 7, open circles). In these experiments, APS was added to the enzyme to form the thiosulfonate enzyme−intermediate. At each time point, an aliquot of the enzyme−intermediate was removed, and 5 nM final concentration was assayed for activity under multiple turnover conditions (e.g., in the presence of thioredoxin). In these reactions, less than 0.05 μM out of a total of 25 μM APS was contributed by the enzyme stock solution. Thus, the stability enhancement was not due to the presence of additional substrate or the 5 nM covalent intermediate that would be reduced during the first turnover. Inclusion of saturating concentrations of AMP also retarded activity loss, though to a lesser extent than addition of APS (Figure 7, closed squares). Addition of millimolar concentrations of sulfite provided no beneficial effects (data not shown). Likewise, no additional stabilization was gained through a combination of AMP and sulfite (data not shown).

To confirm directly that the iron−sulfur cluster was stabilized in the context of the thiosulfonate enzyme−intermediate relative to unbound enzyme, we probed for cluster dissociation using mass spectrometry. The data presented in Figure 8 depict mass spectra of APS reductase in the absence (A) or presence of APS (B). At time zero, all three forms of APS reductase (holo, 2Fe-2S, and apo) were observed in both conditions. In the absence of APS, the iron−sulfur cluster rapidly dissociated from APS reductase, resulting in an ion series with a mass consistent with that of apoprotein (Figure 8A, a−f). In addition, we also observed a series of adducts with a measured mass consistent with the addition of two inorganic sulfides to the protein, +64 Da. Previous studies have also documented the formation of protein−sulfide adducts as a consequence of iron−sulfur cluster breakdown (*17*, *18*). In stark contrast to the rapid cluster decomposition observed in the absence of substrate, the addition of APS (with concomitant formation of the thiosulfonate enzyme−intermediate) prevented dissociation of the iron−sulfur cluster (Figure 8B, a−f). These samples contained two major series of ions that corresponded to the thiosulfonate holoenzyme−intermediate and the thiosulfonate holoenzyme−intermediate bound to AMP; no significant accumulation of the forms of APS reductase lacking a mature cofactor was observed.

DISCUSSION

In this work, a combination of site-directed mutagenesis, spectroscopy, kinetics, and mass spectrometry analysis has provided insight into communication between the enzyme active site and the iron−sulfur cluster in APS reductase. The results affirm the dependence of catalytic reactivity on the iron−sulfur cluster and enable us to propose a more detailed molecular model of how APS reduction might proceed.

Three major results have been obtained in these experiments that underscore the link between APS reductase reactivity and an intact 4Fe-4S cluster: (1) Site-directed mutagenesis studies support a strong correlation between APS reductase activity and iron content, consistent with data obtained with APS reductases from other organisms (*9*, *11*, *22*). (2) Binary complex formation between APS reductase and AMP or thioredoxin, as evaluated by mass spectrometry, indicates that an intact 4Fe-4S cluster is required for ligand interaction. (3) Solution kinetics and mass spectrometry studies demonstrate that formation of the thiosulfonate enzyme−intermediate prevents loss of APS reductase activity and cluster dissociation.

One possible explanation for the lack of ligand binding and catalytic activity in proteins that were not associated with a mature 4Fe-4S cluster is that significant structural perturbation could occur upon cofactor dissociation. For example,

loss of cluster could result in unfolding and denaturation of APS reductase. Admittedly, in the absence of high-resolution structural information this question is difficult to address experimentally. However, to gain some insight into the structural role of the iron−sulfur cluster, we have used circular dichroism to analyze the secondary structure of wild-type and APS reductase variants. When analyzed on a time scale of hours, these studies did not reveal significant secondary structure perturbation in proteins that incorporated reduced levels of iron relative to wild-type APS reductase. In contrast, apoprotein analyzed after several days of incubation at room temperature did exhibit significant unfolding. It is likely that this structural instability is due to protein aggregation over time, perhaps through the formation of nonspecific disulfide bonds. This hypothesis would be consistent with the gel filtration profiles of the variants discussed in the Results section above. In this study, activity and binding experiments were carried with protein that migrated at its expected molecular mass on a size-exclusion column. Additionally, protein was used in experiments immediately after sample preparation. For these reasons, it is unlikely that the lack of reactivity and binding are due to the gross secondary structural perturbation characteristic of aggregated, unfolded protein. Furthermore, although circular dichroism is less adept at detecting more subtle conformational rearrangements, a purely structural role for the cluster in maintaining active site integrity appears unlikely given that, in the absence of any ligand, the cluster itself is prone to degradation.

In this study, we observed that changing any cysteine to serine within the cluster motif yields protein that lacks iron and detectable catalytic activity. These observations are consistent with a role for each cysteine in cluster coordination. However, other studies have reported a larger fraction of iron associated with C141S (using *M. tuberculosis* APS reductase numbering) relative to the other variants and have therefore concluded that this cysteine was not a cluster ligand, proposing instead that C141 formed an intramolecular disulfide bond with C249 (*9*, *10*). In addition to differences in protein preparation detailed above in the Results section, it is also possible that the oligomerization state of APS reductase plays a role in iron−sulfur cluster stability. *A. thaliana* and *P. aeruginosa* APS reductases are isolated as homodimers and homotetramers, respectively (*8*, *9*). In contrast, APS reductase from *M. tuberculosis* and other related organisms such as *Mycobacterium smegmatis* and *Rhizobium meliloti* are monomers (*8*). It is quite plausible that subunit−subunit contacts in homooligomeric APS reductases help to mitigate the loss of C141 and stabilize the iron−sulfur cluster. Moreover, in different macromolecular contexts, it is also possible that either a serine at position 141 could participate in cluster coordination via the O^{γ} atom or a rearrangement of protein structure could occur to promote cluster retention as observed previously for *Azotobacter vinelandii* ferredoxin I (*23*, *24*). Finally, while *P. aeruginosa* C141S is associated with a higher degree of iron and sulfide than the other variants, this same study also reports that the iron−sulfur cluster was less stable in this protein (*10*). Thus, while this residue might not be essential for cluster assembly in *P. aeruginosa* APS reductase, it is clearly essential for cluster retention and stability.

Since results from site-directed mutagenesis can clearly lead to different functional consequences with respect to the coordination of iron−sulfur clusters (*8*, *25*), as an independent test of our mutagenesis data we have performed cysteine-labeling experiments. In the presence of the iron−sulfur cluster only two out of six possible cysteines in *M. tuberculosis* APS reductase were alkylated, C59 and C249. However, removal of the iron−sulfur cluster with the iron chelator OBP permitted the alkylation of the remaining four putative cluster ligands. Taken together, the site-directed mutagenesis and cysteine-labeling data both support a role for all four cysteines within the cluster motif in iron coordination.

Notably, there are no examples of a sequence motif with two adjacent cysteines that bind discrete irons of a 4Fe-4S cluster in the Protein Data Bank. While this arrangement is likely to be under some conformational strain, a recent computational study suggests that it is possible for two vicinal cysteines to coordinate discrete irons within a 4Fe-4S cluster (*26*). In addition, the dicysteine motif is not confined to members of the APS reductase family. This sequence has been identified in other iron−sulfur proteins such as the NuoB subunit of respiratory complex I, *Aquifex aeolicus* hydrogenase II, and *E. coli* FhuF protein as well as in desulforedoxin and desulfoferrodoxin from sulfate-reducing bacteria (*27*−*30*).

Clues to the possible functional consequences of the dicysteine motif in cluster coordination can be found in the crystal structure of desulforedoxin. In this iron−sulfur protein, a single iron atom is coordinated by four cysteines (two of which are adjacent) and results in a distorted tetrahedral arrangement (*31*). Thus, one possibility is that conformational strain necessitated by coordination to a cysteine dyad could promote unique iron−sulfur cluster geometry. Extending this analogy to APS reductase, interaction of the two adjacent cysteines with the 4Fe-4S cluster could provide a way to structurally and functionally distinguish one iron site from the other three in the cluster. This hypothesis would be consistent with the unique EPR and Mössbauer parameters observed in APS reductase and other iron−sulfur proteins with the dicysteine motif (*6*, *9*, *10*, *30*). Furthermore, the recent finding that an iron atom can be selectively ejected from the 4Fe-4S cluster of *P. aeruginosa* APS reductase using the chemical oxidant potassium ferricyanide is also consistent with a distinct iron site within the cluster (*10*).

In this work, we have also demonstrated that ligand binding and thiosulfonate intermediate formation directly impact the stability of the iron−sulfur cluster as well as the reactivity of its cysteine ligands. These data strongly suggest that the enzyme active site is able to communicate with the iron−sulfur cluster. One possibility is that ligand binding results in a conformational change that is transmitted to the cluster through the polypeptide chain. Alternatively, conformational change at the active site could be communicated with the cofactor via a direct interaction between the substrate and the iron−sulfur cluster. On the basis of the vicinity of the enzyme active site to the location of the iron−sulfur cluster predicted by structural homology modeling of APS reductase (K. Carroll, unpublished observation), the second scenario is structurally plausible. Moreover, formation of the covalent intermediate also favors this proposal, as this state

Scheme 3: Proposed Role of the Iron−Sulfur Cluster in APS Reduction

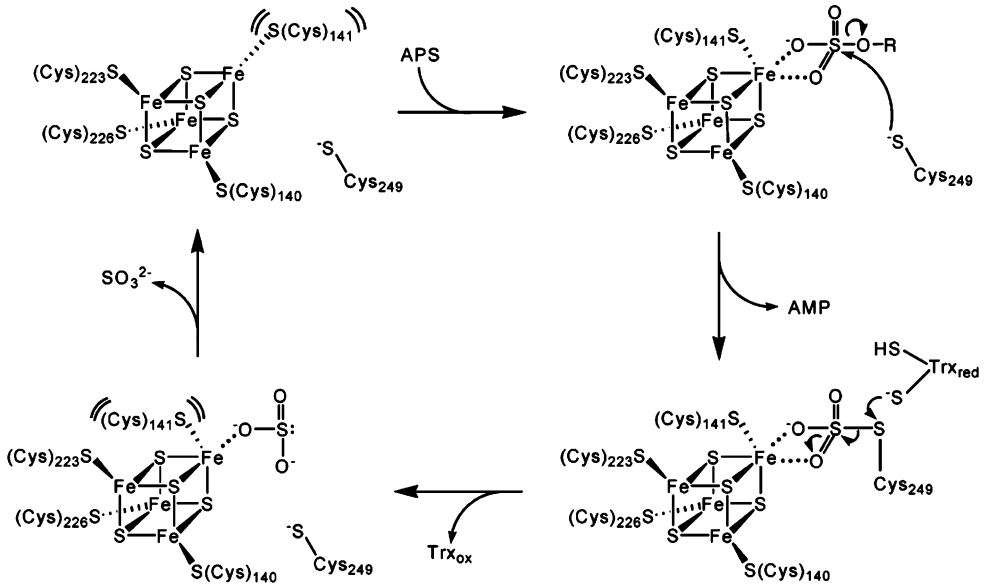

would be highly cross-linked with covalent bonds, restricting the positions of the residues (i.e., protein−C249−sulfite−Fe cluster−cysteines−protein) and could account for the observed increase in cluster stability.

The data presented in this work demonstrate that the iron−sulfur cluster is an integral constituent of the APS reductase active site. Since a purely structural role appears unlikely, what might the functional implications of this arrangement be? One possibility is that the iron−sulfur cluster contributes to substrate binding via electrostatic interaction. With respect to this model, it is interesting to note that the homologous PAPS reductases have lost the iron−sulfur cofactor through divergent evolution. In this context it is plausible that PAPS reductases compensate for the lack of cofactor through the binding energy afforded by the addition of a 3′-phosphate group on the substrate. Another possible model is that the iron−sulfur cluster participates directly in APS reduction (Scheme 3). In the free enzyme, ligation of adjacent cysteines to discrete irons within the cluster could impart a measure of conformational strain at these two sites. This conformational strain could serve as a mechanism to functionalize one iron site within the cluster so that it is poised to interact with the incoming substrate. When APS binds, the terminal sulfate oxygens could interact with this unique iron. The coordinating cysteine at this iron site could remain bound and rearrange to accommodate the increased coordination sphere. Alternatively, this cysteine could shift away from the iron and temporarily interact with a neighboring sulfide or protein residue. To facilitate reduction of APS, the interacting iron might serve as a Lewis acid that activates the substrate for nucleophilic attack and also stabilizes the developing negative charge. In subsequent steps, thioredoxin mediates the reduction of the thiosulfonate enzyme−intermediate (*8*). Return of the vicinal cysteines to their original position due to interaction with thioredoxin and/or AMP release could assist in product formation.

A related role for iron−sulfur cluster participation in substrate binding and activation has been demonstrated for aconitase (*32*). This enzyme contains an iron−sulfur cluster that is coordinated by three cysteine ligands and a hydroxide in the substrate-free state. During the conversion of citrate to isocitrate, the terminal oxygen atoms of the substrate interact with iron atom and the hydroxide becomes protonated, maintaining the overall charge balance of the cluster. However, due to the unique cysteine arrangement, the iron−sulfur cluster of APS reductase appears to be distinct from aconitase. In the case of APS reductase, having an activated water or hydroxide as the fourth ligand would not make good chemical sense. This is because the competing, and more energetically favorable, reaction is the hydrolysis of APS to form sulfate and AMP. Moreover, coordination of a tetrahedral sulfonate differs structurally from a planar carboxyl group in citrate; a sulfonate group is bulkier and could necessitate structural rearrangement of the interacting iron in the covalent intermediate relative to the free enzyme. It is possible, then, that nature has selected a fourth cysteine, in the context of a cysteine dyad, as the fourth cluster ligand in order to stymie the competing reaction and also to facilitate rearrangement of the coordinating ligands upon substrate binding.

While aspects of the model proposed in Scheme 3 will require further experimental confirmation, the absolute conservation of the cysteine dyad and their joint coordination of the cluster strongly suggest a functional basis for its retention. It is possible that this sequence motif is retained in order to accommodate structural or folding constraints. However, this model seems unlikely, as nature has demonstrated repeatedly that a vast array of sequence solutions exists for a single structural problem (*33*). As our ability to characterize iron−sulfur proteins has grown, so too has the discovery of new iron−sulfur cluster functions, for example, in enzymes such as ferrodoxin−thioredoxin reductase as well as in members of the radical−SAM protein superfamily (*34*−*37*). Indeed, the continued discovery of novel iron-containing clusters unique from the standpoint of geometry and atom composition underscores the exciting functional diversity that is possible with these cofactors (*34*).

ACKNOWLEDGMENT

We thank C. David Stout and K. Karbstein for helpful discussions and comments on the manuscript.

REFERENCES

1. Mougous, J. D., Leavell, M. D., Senaratne, R. H., Leigh, C. D., Williams, S. J., Riley, L. W., Leary, J. A., and Bertozzi, C. R. (2002) Discovery of sulfated metabolites in mycobacteria with a genetic and mass spectrometric approach, *Proc. Natl. Acad. Sci. U.S.A. 99*, 17037−17042.
2. Mougous, J. D., Petzold, C. J., Senaratne, R. H., Lee, D. H., Akey, D. L., Lin, F. L., Munchel, S. E., Pratt, M. R., Riley, L. W., Leary, J. A., Berger, J. M., and Bertozzi, C. R. (2004) Identification, function and structure of the mycobacterial sulfotransferase that initiates sulfolipid-1 biosynthesis, *Nat. Struct. Mol. Biol. 11*, 721−729.
3. Williams, S. J., Senaratne, R. H., Mougous, J. D., Riley, L. W., and Bertozzi, C. R. (2002) 5′-Adenosinephosphosulfate lies at a metabolic branch point in mycobacteria, *J. Biol. Chem. 277*, 32606−32615.
4. Sassetti, C. M., Boyd, D. H., and Rubin, E. J. (2001) Comprehensive identification of conditionally essential genes in mycobacteria, *Proc. Natl. Acad. Sci. U.S.A. 98*, 12712−12717.
5. Berendt, U., Haverkamp, T., Prior, A., and Schwenn, J. D. (1995) Reaction mechanism of thioredoxin: 3′-phospho-adenylylsulfate reductase investigated by site-directed mutagenesis, *Eur. J. Biochem. 233*, 347−356.
6. Kopriva, S., Büchert, T., Fritz, G., Suter, M., Benda, R., Schünemann, V., Koprivova, A., Schürmann, P., Trautwein, A. X., Kroneck, P. M., and Brunold, C. (2002) The presence of an iron−sulfur cluster in adenosine 5′-phosphosulfate reductase separates organisms utilizing adenosine 5′-phosphosulfate and phosphoadenosine 5′-phosphosulfate for sulfate assimilation, *J. Biol. Chem. 277*, 21786−21791.
7. Schwenn, J. D., Krone, F. A., and Husmann, K. (1988) Yeast PAPS reductase: properties and requirements of the purified enzyme, *Arch. Microbiol. 150*, 313−319.
8. Carroll, K. S., Gao, H., Chen, H., Stout, C. D., Leary, J. A., and Bertozzi, C. R. (2005) A conserved mechanism for sulfonucleotide reduction, *PLoS Biol. 3*, 250.
9. Kopriva, S., Büchert, T., Fritz, G., Suter, M., Weber, M., Benda, R., Schaller, J., Feller, U., Schürmann, P., Schünemann, V., Trautwein, A. X., Kroneck, P. M., and Brunold, C. (2001) Plant adenosine 5′-phosphosulfate reductase is a novel iron−sulfur protein, *J. Biol. Chem. 276*, 42881−42886.
10. Kim, S. K., Rahman, A., Bick, J. A., Conover, R. C., Johnson, M. K., Mason, J. T., Hirasawa, M., Leustek, T., and Knaff, D. B. (2004) Properties of the cysteine residues and iron−sulfur cluster of the assimilatory 5′-adenylyl sulfate reductase from *Pseudomonas aeruginosa*, *Biochemistry 43*, 13478−13486.
11. Berndt, C., Lillig, C. H., Wollenberg, M., Bill, E., Mansilla, M. C., de Mendoza, D., Seidler, A., and Schwenn, J. D. (2004) Characterization and reconstitution of a 4Fe-4S adenylyl sulfate/phosphoadenylyl sulfate reductase from *Bacillus subtilis*, *J. Biol. Chem. 279*, 7850−7855.
12. Beinert, H. (1978) Micro methods for the quantitative determination of iron and copper in biological material, *Methods Enzymol. 54*, 435−445.
13. Kennedy, M. C., Kent, T. A., Emptage, M., Merkle, H., Beinert, H., and Munck, E. (1984) Evidence for the formation of a linear [3Fe-4S] cluster in partially unfolded aconitase, *J. Biol. Chem. 259*, 14463−14471.
14. Plank, D. W., Kennedy, M. C., Beinert, H., and Howard, J. B. (1989) Cysteine labeling studies of beef heart aconitase containing a 4Fe, a cubane 3Fe, or a linear 3Fe cluster, *J. Biol. Chem. 264*, 20385−20393.
15. Pramanik, B. N., Bartner, P. L., Mirza, U. A., Liu, Y. H., and Ganguly, A. K. (1998) Electrospray ionization mass spectrometry for the study of non-covalent complexes: an emerging technology, *J. Mass Spectrom. 33*, 911−920.
16. Veenstra, T. D. (1999) Electrospray ionization mass spectrometry: a promising new technique in the study of protein/DNA noncovalent complexes, *Biochem. Biophys. Res. Commun. 257*, 1−5.
17. Hernandez, H., Hewitson, K. S., Roach, P., Shaw, N. M., Baldwin, J. E., and Robinson, C. V. (2001) Observation of the iron−sulfur cluster in *Escherichia coli* biotin synthase by nanoflow electrospray mass spectrometry, *Anal. Chem. 73*, 4154−4161.
18. Johnson, K. A., Verhagen, M. F., Brereton, P. S., Adams, M. W., and Amster, I. J. (2000) Probing the stoichiometry and oxidation states of metal centers in iron−sulfur proteins using electrospray FTICR mass spectrometry, *Anal. Chem. 72*, 1410−1418.
19. Abola, A. P., Willits, M. G., Wang, R. C., and Long, S. R. (1999) Reduction of adenosine-5′-phosphosulfate instead of 3′-phosphoadenosine-5′-phosphosulfate in cysteine biosynthesis by *Rhizobium meliloti* and other members of the family Rhizobiaceae, *J. Bacteriol. 181*, 5280−5287.
20. Hausinger, R. P., and Howard, J. B. (1983) Thiol reactivity of the nitrogenase Fe-protein from *Azotobacter vinelandii*, *J. Biol. Chem. 258*, 13486−13492.
21. Weber, M., Suter, M., Brunold, C., and Kopriva, S. (2000) Sulfate assimilation in higher plants: Characterization of a stable intermediate in the adenosine 5′-phosphosulfate reductase reaction, *Eur. J. Biochem. 267*, 3647−3653.
22. Suter, M., von Ballmoos, P., Kopriva, S., den Camp, R. O., Schaller, J., Kuhlemeier, C., Schürmann, P., and Brunold, C. (2000) Adenosine 5′-phosphosulfate sulfotransferase and adenosine 5′-phosphosulfate reductase are identical enzymes, *J. Biol. Chem. 275*, 930−936.
23. Martin, A. E., Burgess, B. K., Stout, C. D., Cash, V. L., Dean, D. R., Jensen, G. M., and Stephens, P. J. (1990) Site-directed mutagenesis of *Azotobacter vinelandii* ferredoxin I: [Fe-S] cluster-driven protein rearrangement, *Proc. Natl. Acad. Sci. U.S.A. 87*, 598−602.
24. Shen, B., Jollie, D. R., Diller, T. C., Stout, C. D., Stephens, P. J., and Burgess, B. K. (1995) Site-directed mutagenesis of *Azotobacter vinelandii* ferredoxin I: cysteine ligation of the [4Fe-4S] cluster with protein rearrangement is preferred over serine ligation, *Proc. Natl. Acad. Sci. U.S.A. 92*, 10064−10068.
25. Moulis, J. M., Davasse, V., Golinelli, M. P., Meyer, J., and Quinkal, I. (1996) The coordination sphere of iron−sulfur clusters: lessons from site-directed mutagenesis experiments, *J. Bioinorg. Chem. 1*, 2−14.
26. Gurrath, M., and Friedrich, T. (2004) Adjacent cysteines are capable of ligating the same tetranuclear iron−sulfur cluster, *Proteins 56*, 556−563.
27. Brugna-Guiral, M., Tron, P., Nitschke, W., Stetter, K. O., Burlat, B., Guigliarelli, B., Bruschi, M., and Giudici-Orticoni, M. T. (2003) [NiFe] hydrogenases from the hyperthermophilic bacterium *Aquifex aeolicus*: properties, function, and phylogenetics, *Extremophiles 7*, 145−157.
28. Flemming, D., Schlitt, A., Spehr, V., Bischof, T., and Friedrich, T. (2003) Iron−sulfur cluster N2 of the *Escherichia coli* NADH: ubiquinone oxidoreductase (complex I) is located on subunit NuoB, *J. Biol. Chem. 278*, 47602−47609.
29. Matzanke, B. F., Anemuller, S., Schünemann, V., Trautwein, A. X., and Hantke, K. (2004) FhuF, part of a siderophore-reductase system, *Biochemistry 43*, 1386−1392.
30. Müller, K., Matzanke, B. F., Schünemann, V., Trautwein, A. X., and Hantke, K. (1998) FhuF, an iron-regulated protein of *Escherichia coli* with a new type of [2Fe-2S] center, *Eur. J. Biochem. 258*, 1001−1008.
31. Archer, M., Huber, R., Tavares, P., Moura, I., Moura, J. J., Carrondo, M. A., Sieker, L. C., LeGall, J., and Romao, M. J. (1995) Crystal structure of desulforedoxin from *Desulfovibrio gigas* determined at 1.8 Å resolution: a novel non-heme iron protein structure, *J. Mol. Biol. 251*, 690−702.
32. Beinert, H., Kennedy, M. C., and Stout, C. D. (1996) Aconitase as iron−sulfur protein, enzyme, and iron-regulatory protein, *Chem. Rev. 96*, 2335−2374.
33. Fersht, A. (1999) *Structure and Mechanism in Protein Science: A Guide to Enzyme Catalysis and Protein Folding*, W. H. Freeman, New York.
34. Beinert, H. (2000) Iron−sulfur proteins: ancient structures, still full of surprises, *J. Biol. Inorg. Chem. 5*, 2−15.
35. Berkovitch, F., Nicolet, Y., Wan, J. T., Jarrett, J. T., and Drennan, C. L. (2004) Crystal structure of biotin synthase, an S-adenosylmethionine-dependent radical enzyme, *Science 303*, 76−79.
36. Dai, S., Schwendtmayer, C., Schürmann, P., Ramaswamy, S., and Eklund, H. (2000) Redox signaling in chloroplasts: cleavage of disulfides by an iron−sulfur cluster, *Science 287*, 655−658.
37. Staples, C. R., Gaymard, E., Stritt-Etter, A. L., Telser, J., Hoffman, B. M., Schürmann, P., Knaff, D. B., and Johnson, M. K. (1998) Role of the [Fe4S4] cluster in mediating disulfide reduction in spinach ferredoxin:thioredoxin reductase, *Biochemistry 37*, 4612−4620.

BI051344A